Plasmonics (2013) 8:1293–1297
DOI 10.1007/s11468-013-9517-y

Effect of Boundary Condition and Periodical Extension on Transmission Characteristics of Terahertz Filters with Periodical Hole Array Structure Fabricated on Aluminum Slab

JiaMing Xu · Lin Chen · Le Xie · ShaoQing Du · MingHui Yuan · Yan Peng · YiMing Zhu

Received: 13 August 2012 / Accepted: 25 February 2013 / Published online: 23 March 2013

Abstract Terahertz (THz) filters based on extraordinary optical transmission from periodical hole array structures fabricated on aluminum slab have been experimentally investigated by using THz time-domain spectroscopy. The incident THz pulses with frequency from 0.1 to 2.7 THz could be partly filtered, and the central peak was at ~0.26. The high frequency signal could be observed to decrease, especially for the frequency above ~1 THz. Moreover, the transmission peak from small-size sample with less hole arrays shifts to high frequency at ~0.53 THz due to both the effects of boundary condition and insufficient periodical extension. Furthermore, finite element method with surface plasmon polariton theory is employed to analyze this extraordinary optical transmission and filter phenomena.

Keywords Ultrafast optics · Hole array structures · Terahertz time-domain spectroscopy · Surface plasmon polaritons · Finite element method

Introduction

Recently, with the development of terahertz (THz) technology, it is necessary to manufacture THz narrow-bandpass filters for different requirements, i.e., requiring kinds of mono-THz pulse for communication [1] and for bio-chemistry detection [2, 3]. However, up to now, it is still extremely difficult to realize the THz filter with low cost and simple fabrication process. On the other hand, the THz devices with microstructure, i.e., dichroic filters [4, 5] also greatly interest researchers in the extraordinary transmission of electromagnetic waves [6, 7].

In 1998, extraordinary optical transmission has been observed by using two-dimensional (2D) arrays with sub-wavelength holes by Ebbesen et al. [6]. Such extraordinary optical transmission could be applied potentially for tunable filters [8]. As shown in the experiment [6, 8], the extraordinary optical transmission from sub-wavelength hole arrays was observed in the case where no propagation mode should be supported. Furthermore, the transmission frequency corresponds to the surface plasmon polariton (SPP) resonant frequency. This result indicates that the enhanced transmission may be attributed to the interaction of incident light with SPPs [9]. After that, Pendry et al. have shown theoretically that there really exists an SPP-like mode, whose amplitude exponentially decays with increasing the distance from surface on perfect conductor metal surfaces perforated with arrayed holes [10]. They claimed that enhanced transmission from 2D metal hole arrays made on a perfect conductor was caused by these SPP-like modes. It has also been reported that the coupling of the SPP mode and the propagation mode becomes stronger as the thickness decreases and the hole diameter increases [11]. However, there is little work about theoretical and experimental comparison of transmission properties between samples with different size and number of hole arrays in THz region, which is significant for the fabrication of THz filters.

In this paper, we have experimentally studied the transmission properties of terahertz pulses through different sizes

J. Xu · L. Chen · L. Xie · S. Du · M. Yuan · Y. Peng · Y. Zhu (✉)
Engineering Research Center of Optical Instrument and System, Ministry of Education and Shanghai Key Lab of Modern Optical System, University of Shanghai for Science and Technology, Shanghai 200093, China
e-mail: ymzhu@usst.edu.cn

L. Chen
e-mail: linchen@usst.edu.cn

of aluminum slabs perforated by periodical hole array structure in THz range by THz time-domain spectroscopy (THz-TDS). From the experimental results, the incident THz pulses with frequency from 0.1 to 2.7 THz could be partly filtered, and the central peaks were at ~0.53 THz for small-size sample and ~0.26 THz for big-size sample. For both samples, the signals in high frequency range were observed to decrease, especially for the frequency above ~1 THz, which were filtered dramatically. The different results between small-size sample and big-size sample are due to boundary condition and insufficient periodical extension. Furthermore, filter and extraordinary optical transmission phenomena can be explained by SPP theory with the help of finite element method (FEM) analysis. The simulation results show good agreement with experimental results for the big-size sample.

Experiment

The samples used in this work were fabricated by micro-mechanization processing. The structure of 2D metal hole arrays was fabricated on a 0.25-mm-thick aluminum slab, as shown in Fig. 1a. The hole diameter, d, and lattice constant, s, were 0.6 and 1.13 mm, respectively. Figure 1b shows the SEM image of the hole arrays. Figure 1c is the photo image of the small-size sample with 39 holes on 6 mm×6 mm aluminum slab. Figure 1d is the photo image of the big-size sample with more than 5,000 holes on 100 mm×100 mm aluminum slab and margin in the edge of slab, whose size is almost 278 times bigger than the small sample.

In this paper, the THz-TDS was used for the measurement of transmission properties of terahertz pulses through 2D metal hole arrays. A mode-locked Ti/sapphire laser was applied to pump and detect THz wave, with the central wavelength at 800 nm, the full width at half maximum of spectral bandwidth at ~11 nm, pulse duration around 80 fs, repeat frequency at 76 MHz, and output power at 1.1 W. The laser was split into pump and probe beam by beam splitter. Pump beam modulated by optical chopper was focused on Gallium Arsenide (GaAs) *m-i-n* diode. At such condition, electrons were created near the bottom of the conduction band, as well as holes were created near the top of the valence band in intrinsic GaAs layer. The electrons were accelerated by the applied electrical field, and then, THz wave was emitted out [12, 13] from GaAs *m-i-n* diode and focused on sample by two off-axis parabolic mirrors. The waist radius of THz beam is about 3 mm whose size is similar to the small plate. After passing through the sample, the THz wave with the information of the samples and probe beam was focused on zinc telluride electro-optic crystal (ZnTe EO crystal) by another two off-axis parabolic mirrors. The free space EO sampling technique was used to record temporal waveforms of THz electric fields emitted from the samples [14, 15]. The EO detector used in this experiment was a 700-μm-thick<110>-oriented ZnTe crystal. The high frequency cutoff (~3 THz) was determined by the thickness

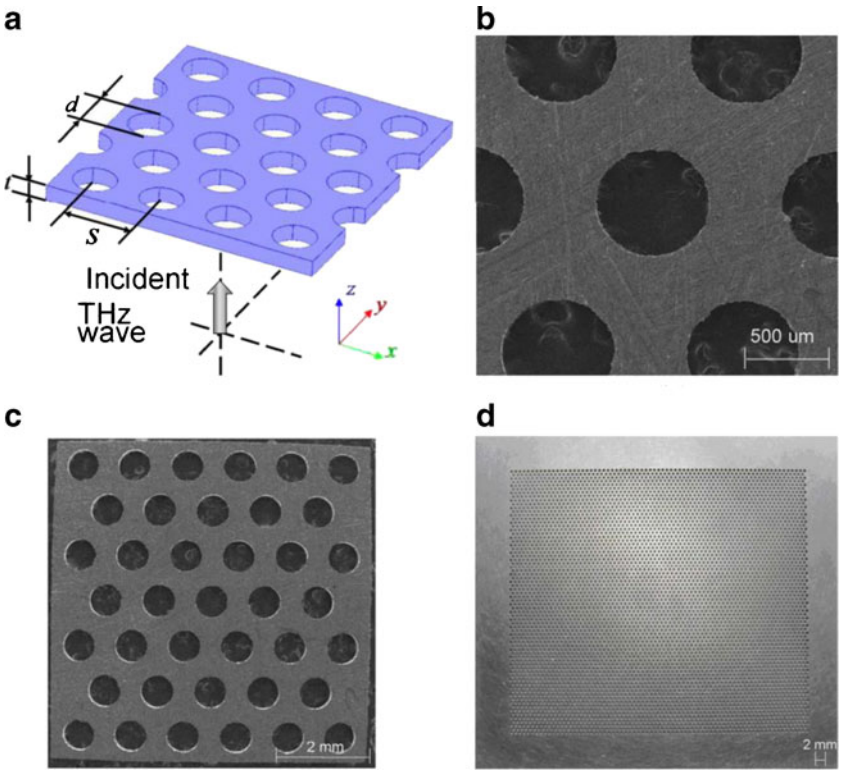

Fig. 1 **a** Schematic of the 2D metal hole arrays. **b** SEM image of hole arrays fabricated on aluminum slab (hole diameter, d=0.7 mm; lattice constant, s=1.13 mm; slab thickness, t=0.25 mm). **c** Photo image of small-size sample with 39 holes on 6 mm×6 mm aluminum slab. **d** Photo image of big-size sample with more than 5,000 holes on 100 mm×100 mm aluminum slab and margin in the edge of slab

of the EO crystal together with the pulse duration of the femtosecond laser [16, 17]. To avoid the strong absorption of water vapor, nitrogen gas was infused into a covered box which covered the main part of THz paths. The humidity of the covered box was kept as less than 8 %, and temperature was in the range from 23.5 to 24.5 °C.

Experiment Results

The reference THz pulses (without samples) and transmitted THz pulses, together with their corresponding spectra, are illustrated in Fig. 2.

Figure 2a, c shows the reference THz signals (red curves) and the THz waveforms transmit through the samples (blue curves) in time domain. It should be noted in Fig. 2 that the position of $t=0$ was carefully determined by the maximum entropy method [18, 19], the detail of which will be reported elsewhere. The estimated time error is less than ±30 fs. Then, from these signals, we can clearly observe that there is no time delay between the reference signal and the THz signals through the samples, which means that the THz pulses can transmit the metal slab.

Furthermore, the amplitude of sample signal decreases as comparing with the reference signal. Also, the main peak of sample signal is broadened, which can be found by observing the first dip in Fig. 2a. The spectra of reference signal (red curve) and the transmitted signal through the small sample (blue curve) are obtained by using Fourier transform, as shown in Fig. 2b. The amplitude of signal in high frequency range decreases, especially for the frequency above ~1 THz. The filtering effect is clearly observed. By comparing with the amplitude of $E_{\mathrm{THz}}(\omega)$ for both the reference signal and the signal from the sample at ~0.53 THz, we can find that the transmission efficiency of THz filter with small-size sample (less periodical hole arrays) can reach almost 90 %.

Figure 2c shows the reference THz signal (red curve) and the THz waveform transmit through the big-size sample (blue curve) in time domain. Similar with the small-size sample case, the amplitude of THz signal through the big-size sample decreases. It is also obvious that five damped oscillations occur after the main peak, whose period is about 3.75 ps. The spectra of reference signal and the transmitted signal from the big-size sample are shown in Fig. 2d. The filtering effect is also clearly observed. The amplitude of signal in high frequency range decreases, especially for the frequency above ~1 THz, which is the same as the small-size sample. By comparing with the amplitude of $E_{\mathrm{THz}}(\omega)$ for both the reference signal and the signal from the big-size sample at 0.26 THz, we can find that the transmission efficiency of big-size sample (more hole arrays) is about 95 %.

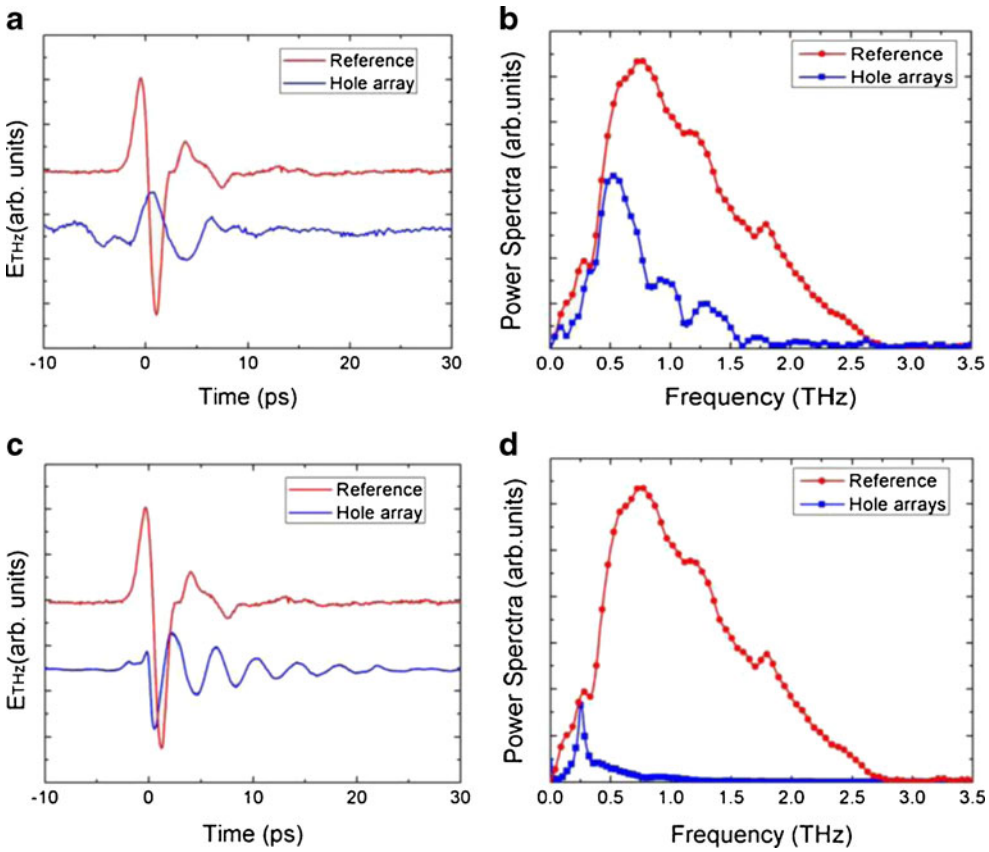

Fig. 2 **a** The reference waveform (*red*) and the transmitted THz wave from small-size sample (*blue*) in time domain. **b** The spectra of reference signal (*red*) and the transmitted signal through small-size sample (*blue*). **c** The reference waveform (*red*) and the transmitted THz wave from big-size sample (*blue*) in time domain. **d** The spectra of reference signal (*red*) and the transmitted signal through big-size sample (*blue*)

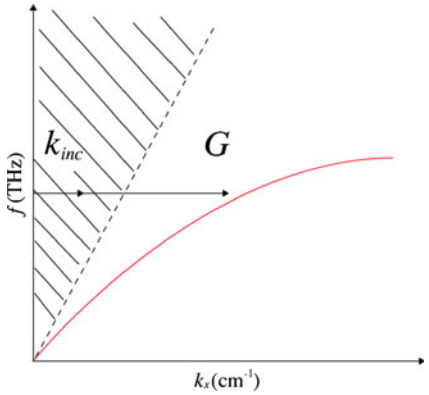

Fig. 3 The illustration of the dispersion curve of light and SPs. The *dotted line* corresponds to the dispersion curve of light. The *hatched sector* corresponding the dispersion curve of propagating waves does not overlap with the *evanescent sector*, which contains the SPs mode, below the dispersion curve of light marked as *dash line*. k_{inc} is the transverse component of incident wave vector, and G corresponds to the momentum needed for coupling to SP mode in the *evanescent sector*

Theoretical Analysis

For theoretical analysis, the Drude model is employed to analyze the surface plasmons (SPs) occurring at the interface with a dielectric layer (permittivity, ε_d) and a metal layer (permittivity, ε_m). Such a model is characterized by a wave vector of SPs which can be described by the following equation [19]

$$k_{sp} = \frac{\omega}{c}\sqrt{\frac{\varepsilon_d \varepsilon_m}{\varepsilon_d + \varepsilon_m}} \tag{1}$$

Here, ω is the angle frequency of electromagnetic field, and c is the velocity of light in vacuum. The red curve in Fig. 3 shows the dispersion curve of SPs on the interface between metal layer and dielectric layer.

SPs can be resonantly excited by the coupling of incident electromagnetic field and free surface charges from metal. However, in real case, SP modes cannot be generated because the wave vector of SPs, k_{sp}, is below the dispersion of light. This implies that such mode is evanescent and, therefore, cannot be excited directly from free-propagating light. A given additional momentum G is needed to let the wave vector of the incident light, k_{inc}, fall into the evanescent sector for momentum conservation, where SP modes can exist and transmit on the surface of metal.

One simple way is to provide a momentum G for coupling incoming light to generate SPs by a periodical array. In two dimension case, G can be divided into G_x and G_y along the x direction and y direction, respectively, which should be the integer multiple of $2\pi/a_0$ where a_0 is the period of artificial structure. When incident angle of light is θ, we can obtain [20]

$$k_{sp} = k_{inc} + i \times G_x + j \times G_y = k_0 \sin\theta + (i+j)\frac{2\pi}{a_0} \tag{2}$$

Periodic metallic structures can convert light into SPs by providing the additional momentum for the coupling process by using artificial array. When light inputs on the surface, the transmission processes can be divided into three steps: the light couples to SPs on the incident surface, transmits through the holes to the back surface with SPs mode, and then re-emits from the back surface. Only the selective frequency can pass the metallic slab with hole arrays by experiencing the processes as mentioned above.

For quantitative analysis, the filter phenomenon, as shown in Fig. 2b, d, the time-harmonic Maxwell's equations from SPP theory for describing the processes of light transmission and scattering are employed by using FEM. We set transverse magnetic wave as incident light in the real case in our experiment. Furthermore, ε_d=1 and ε_m=−5.1069×104+ i×1.2061×106 are applied for the permittivity of vacuum and aluminum slab in THz range, respectively. We also use perfectly matched layer (PML) around the slab sample as boundary condition by assuming that there is no reflected light. Figure 4 shows the simulation result, marked as red curve, which matches the experimental result of big-size sample well.

We can clearly see the difference between the simulated and experimental results of small sample from Fig. 4a and good agreement between the simulated and experimental

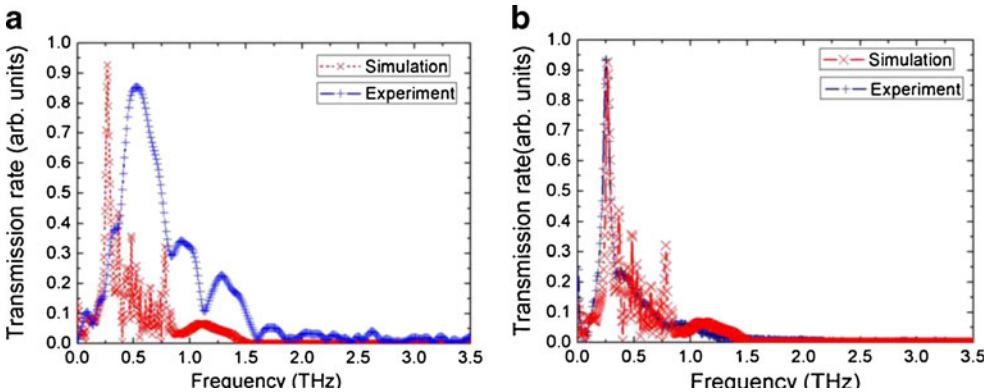

Fig. 4 The comparison between calculated and experimental results. The *blue curve* is the experimental results, and the *red curve* is the simulated results by using FEM. **a** Small-size sample. **b** Big-size sample

results of big-size sample in Fig. 4b. The main peak of small-size sample from simulation is about 0.26 THz and from experiment is around 0.53 THz. This is probably due to the stretching limit of periodical hole array structures and the finite boundary. For small sample, from the central hole of the structures, there are only three rings composed by 6, 12, and 16 holes distribute on the surface, leading to insufficient periodical extension with only three periodical structures. Moreover, in small-size sample case, we manufacture the sample whose size is similar to the waist radius of THz beam, which causes serious problems. Our THz emitter is a dipole source. High frequency signals are in the central area and low frequency signals distribute dispersedly around. From our calculation, the signals below 0.6 THz have opportunities to go through the small sample directly from the edge of structure. Therefore, as the waist radius of THz beam is similar to the small plate, the final signal should be the superposition of part of original wave and filtered signal, whose central frequency is submerged in ~0.53 THz. Furthermore, we also use PML condition around the structure in our simulation, which means we extend the structure to be infinity for preventing wave reflecting. Then, the SPs cannot leak from the boundaries. This phenomenon is also difficult for the real experimental case, especially for the small sample. In contrast, the big-size sample has more hole arrays and enough margin in the edge of sample, providing sufficient periodical extension and nearly infinite boundary condition, which can prevent the original wave transmitting through the sample and is similar to the PML condition. We believe that these two problems mainly result in the different filtered signals from small and large plates. However, the quantity calculation is almost impossible using the current computer, owing to the extremely large memory requirement and computing time

Conclusion

In conclusion, we fabricated the hole array structures on aluminum slab and used THz-TDS to perform the transmission properties of THz waves. From the experimental results, the filter phenomenon is observed. THz pulses in frequency range from 0.1 to 2.7 THz can be filtered, and the central peaks are at ~0.53 THz for small-size sample and ~0.26 THz for big-size sample, respectively. The transmitted signals in high frequency range could be observed to decrease, especially for the frequency above ~1 THz. Furthermore, simulation with the same structures of slab is done by using FEM with SPP theory. Comparing with the experimental results, the theoretical simulations show good fit with experimental results for the big-size sample. The difference between the calculated and experimental results of small-size sample mainly comes from the insufficient periodical extension and boundary condition.

Acknowledgments This work is supported by Ministry of Education Doctoral Fund of new teachers of China (20093120120007), Shanghai Committee of Science & Technology (11ZR1425000), Ministry of Education Scientific Research Foundation for Returned, and National Natural Science Foundation of China (61007059, 11174207, 61138001 and 61205094).

References

1. Kitaeva GK (2008) Terahertz generation by means of optical lasers. Laser Phys Lett 5(8):559–576
2. Federici JF, Schulkinm B, Huang F, Gary D, Barat R, Oliveira F, Zimdars D (2005) THz imaging and sensing for security applications—explosives, weapons and drugs. Semicond Sci Technol 20: S266–S280
3. Rogalski A (2003) A. Infrared photodetectors: status and trends. Prog Quantum Electron 27(2–3):59–210
4. Zhang H, Guo P, Chang SJ, Yuan JH (2008) Magnetically tunable terahertz switch and band-pass filter. Chin Phys Lett 25(11):3898–3900
5. Baumann F, Bailey WA, JrA N, Goodhue WD, Gatesman AJ (2003) Wet-etch optimization of free-standing terahertz frequency-selective structures. Opt Lett 28:938
6. Ebbesen TW, Lezec HJ, Ghaemi HF, Thio T, Wolff PA (1998) Extraordinary optical transmission through sub-wavelength hole arrays. Nature 391:667–669
7. Grupp DE, Lezec HJ, Ebbesen TW, Pellerin KM, Thio T (2000) Crucial role of metal surface in enhanced transmission through subwavelength apertures. Appl Phys Lett 77:1569–1571
8. Barnes WL, Dereux A, Ebbesen TW (2003) Surface plasmon subwavelength optics. Nature 424:824–830
9. Degiron A, Lezec HJ, Barnes WL, Ebbesen TW (2002) Effects of hole depth on enhanced light transmission through subwavelength hole arrays. Appl Phys Lett 81:4327
10. Pendry JB, Martín-Moreno L, García-Vidal FJ (2004) Mimicking surface plasmons with structured surfaces. Science 305:847
11. Genet C, van Exter MP, Woerdman JP (2003) Fano-type interpretation of red shifts and red tails in hole array transmission spectra. Opt Commun 225:331
12. Zhu YM, Unuma T, Shibata K, Hirakawa K (2008) Power dissipation spectra and terahertz intervalley transfer gain in bulk GaAs under high electric fields. Appl Phys Lett 93:232102
13. Shi W, Jia WL, Hou L, Xu JZ, Zhang XC (2004) Investigation on terahertz generation with GaAs photoconductor triggered by femtosecond laser pulse. Chin Phys Lett 21(9):1842–1844
14. Planken PCM, Nienhuys HK, Bakker HJ, Wenckebach T (2001) Measurement and calculation of the orientation dependence of terahertz pulse detection in ZnTe. J Opt Soc Am B 18:313
15. Zang LL, Zhao GZ, Zhong H, Hu Y, Zhang CL (2004) Time-resolved terahertz spectroscopy with free-space electro-optic sampling. Chin Phys Lett 21(11):2295–2297
16. Wu Q, Zhang XC (1997) Free-space electro-optics sampling of mid-infrared pulses. Appl Phys Lett 70:1784
17. Leitenstorfer A, Hunsche S, Shah J, Nuss MC, Knox WH (1999) Femtosecond charge transport in polar semiconductors. Appl Phys Lett 74:1516
18. Vartiainen EM, Ino Y, Shimano R, Kuwata-Gonokami M, Svirko YP, Peiponen KE (2004) Numerical phase correction method for terahertz time-domain reflection spectroscopy. J Appl Phys 96:4171
19. Genet C, Ebbesen TW (2007) Light in tiny holes. Nature 445:39–46
20. Raether H (1998) Surface plasmons on smooth and rough surfaces and on gratings. Springer-Verlag, Berlin